GEOTAIL, POLAR, AND WIND OBSERVATIONS OF AURORAL KILOMETRIC RADIATION

Roger R. Anderson[2,1], Hiroshi Matsumoto[2], Kozo Hashimoto[2], Hirotsugu Kojima[2], Yasumasa Kasaba[3], Michael L. Kaiser[4], Jean-Louis Bougeret[5], Jean-Louis Steinberg[5], and Gordon Rostoker[6]

[1] *Department of Physics and Astronomy, The University of Iowa, Iowa City, IA 52242-1479, USA*
[2] *Radio Science Center for Space and Atmosphere, Kyoto University, Gokanosho, Uji, Kyoto 611-0011, Japan*
[3] *The Institute of Space and Astronautical Science, 3-1-1, Yoshinodai, Sagamihara, Kanagawa 229, Japan*
[4] *NASA/Goddard Space Flight Center, Laboratory for Extraterrestrial Physics, Code 695, Greenbelt, MD, 20771, USA*
[5] *Observatoire de Paris, LESIA/CNRS, 5, Place Jules Janssen, 92195 Meudon, France*
[6] *Department of Physics, University of Alberta, Edmonton, Alberta, Canada T6G 2Jl*

ABSTRACT

Auroral kilometric radiation (AKR) is the plasma wave/radio phenomenon most clearly associated with substorms and increased geomagnetic activity. The GEOTAIL and POLAR Plasma Wave Instruments (PWI) both included sweep frequency receivers that had an upper frequency limit of 800 kHz and the WIND WAVES Thermal Noise Receiver (TNR) and Radio Receiver Band 1 (RAD1) went to 256 kHz and 1024 kHz, respectively. We have thus been able to observe the majority of the AKR spectrum in better detail than with earlier instrumentation and many important new discoveries have been made. Terrestrial low frequency (LF) bursts are a part of AKR observed during strong substorms. Although a limited portion of the LF burst spectrum is often detected on the dayside of the Earth and in the upstream solar wind, the complete spectrum is most frequently detected by spacecraft in the nightside magnetosphere or geomagnetic tail. Frequently these observations show that the LF bursts have a tapered tail centered on the present or recent past solar wind plasma frequency. We have found that on the dayside and in the upstream solar wind the high frequency AKR is detected during LF burst events only if the path from the AKR source is not blocked by the earth or dense plasmasphere. POLAR observations from high over the AKR source region show that the AKR increases in intensity and its lower frequency limits decrease when LF bursts are observed indicating that the AKR source region is expanding to higher altitudes. Frequently the upper frequency limit also increases indicating that the source region is then also expanding to lower altitudes. Data from both satellite and ground-based experiments show that the LF bursts are well correlated with expansive phase onsets and occur during very geomagnetically-disturbed periods. High resolution (in both time and frequency) data from the POLAR Wide Band Receiver have yielded exciting data on the fine structure of AKR as well as details on the structure of LF bursts.

INTRODUCTION

Plasma wave and radio measurements from the GEOTAIL, POLAR, and WIND spacecraft which were a part of the International Solar Terrestrial Physics/Global Geospace Science (ISTP/GGS) program (Acuna et al., 1995) have provided both in situ and remote observations of numerous plasma wave phenomena related to geomagnetic storms and substorms. Observations of auroral kilometric radiation (AKR) (Gurnett, 1974; Voots et al., 1977; Kaiser and Alexander, 1977b), the phenomenon most clearly associated with substorms and increased geomagnetic activity, provide remote or in situ (depending on the orbit) indicators of the timing, dynamics, and strengths of geomagnetic storms and substorms as well as characteristics of the source region and the generation mechanisms. The ISTP/GGS spacecraft were well instrumented to advance our understanding of AKR and related phenomena (Anderson et al., 1997, 1998, 2001). The GEOTAIL Plasma

Wave Instrument (PWI) (Matsumoto et al., 1994) included a sweep frequency analyzer (SFA) that went up to 800 kHz with a sweep period of 8 seconds and a multichannel analyzer (MCA) that went up to 311 kHz and could produce a spectrum every 1/4 second. The POLAR PWI (Gurnett et al., 1995) included sweep frequency receivers (SFR) that also went up to 800 kHz with a sweep period of 2.4 seconds and an MCA that went up to 311 kHz and produced a spectrum every 1.3 seconds. The POLAR PWI also included a Wide Band Receiver (WBR) that provided both high-time resolution and high-frequency resolution data (up to 249,000 samples per second) with up to a 90 kHz bandwidth and a translatable frequency offset covering much of the AKR spectrum. The radio science experiment WAVES on WIND (Bougeret et al., 1995) included a Thermal Noise Receiver (TNR) that covered 4 kHz to 256 kHz and a Radio Receiver Band 1 (RAD1) that went to 1024 kHz but both had somewhat poorer time resolution than GEOTAIL or POLAR.

The initiation or intensification of AKR occurs coincident with substorm onset. Fairfield et al., (1998,1999) showed that AKR onsets and intensifications observed by WIND WAVES, GEOTAIL PWI, and POLAR PWI were coincident and closely associated with high-velocity earthward flow bursts in the inner magnetotail identified with substorm onset. In order to calculate the sizes of plasmoids and the locations of the near-Earth X-line, Murata et al. (1995) used GEOTAIL PWI AKR observations to identify substorm onset (and the release or initiation of plasmoid flow) and in situ measurements of the magnetic fields from the GEOTAIL Magnetic Field Experiment (MGF) (Kokubun et al., 1994) and magnetic noise bursts from the MCA data to determine the timing of the passage of a plasmoid/flux rope over the spacecraft. Liou et al. (1999) in an investigation of relative timing in substorm signatures found that the start of enhanced AKR observed by POLAR when the spacecraft was in the midnight sector was coincident with a sudden auroral brightening indicative of an auroral breakup. These and other studies have shown that for spacecraft with an adequate view of the auroral zone, the initiation or intensification of AKR can be a very accurate identifier of substorm onset.

A 38-month data set of GEOTAIL plasma wave observations of AKR from 100 kHz to 600 kHz was used by Kasaba et al. (1997) to examine the dependence of the angular distribution of AKR. While Green et al. (1977) and Green and Gallagher (1985) had found using the IMP-6 and Hawkeye MCA data (with a 178 kHz upper frequency limit) that the AKR illumination pattern broadens with increasing frequency from 56.2 kHz to 178 kHz, Kasaba et al. (1997) found using the GEOTAIL SFA data (with a 800 kHz upper frequency limit) that the AKR illumination pattern then becomes narrower above 300 kHz. Such differences are basically explained by propagation. The GEOTAIL study also found that the illumination region of AKR extends duskward as geomagnetic conditions become more disturbed especially for the low frequency range which suggests a duskward extension of the AKR source. Kasaba et al. (1997) speculated that the lack of such a feature in the high frequency range could be caused by insufficient density depression in the duskside auroral plasma cavity especially at lower altitudes. Hashimoto et al. (1998) compared AKR simultaneously observed by GEOTAIL PWI and WIND WAVES and found using ray tracing that most observations were explained by an AKR source around 21-22 MLT (Magnetic Local Time) but during substorms the source extended around to 19 MLT.

Several studies using the POLAR and/or GEOTAIL PWI measurements in comparison with data from the POLAR imaging experiments have shown clear associations between electron precipitation and AKR. Plasma wave and bremsstrahlung x-ray data from the POLAR PWI and PIXIE (Imhof et al., 1995) experiments were used by Imhof et al. (1998) to find a 0.51 correlation coefficient over a six hour local time range in the pre-midnight sector for a satellite pass that had several short term enhancements in the intensities of both AKR waves from 60 kHz to 800 kHz and 2 to 12 keV x-ray emissions. Other POLAR PWI and PIXIE (Imhof et al., 1999; 2000) and GEOTAIL PWI and PIXIE (Imhof et al., 2001) correlative studies found that the cross-correlation coefficient of auroral x-rays and AKR emissions was enhanced over an MLT interval of six hours or less and the maximum occurred for x-rays emitted slightly before local midnight. In another GEOTAIL PWI and PIXIE correlative study of the dependence of AKR production on the intensity and energy spectra of auroral bremsstrahlung x-rays, Imhof et al. (2003) found that the x-rays with higher e-folding energy were correlated with higher AKR frequency (implying lower altitude of generation). This was interpreted as being due to the increased energy of the primary electrons resulting from acceleration through an increasing potential difference at lower altitude. Imhof et al. (2003) also found that higher x-ray fluxes were associated with lower AKR cutoff frequencies. The primary generation mechanism presently

considered for AKR, the electron cyclotron maser instability (Wu and Lee, 1979), requires a small plasma frequency to cyclotron frequency ratio. AKR is generated near the local electron cyclotron frequency Fce such that high frequency AKR is generated at a lower altitude than the low frequency AKR. High time and frequency resolution measurements by the FAST satellite have confirmed that the AKR source is in a density depleted cavity and the AKR emissions are very close to and sometimes slightly below the cold plasma Fce down to the relativistic Fce (Ergun et al., 1998). The frequency of AKR thus identifies the location along a magnetic field line where it is generated. For example, on a 71 degree invariant latitude (L=9.4) field line typical for an AKR source region, Fce equals 500 kHz at a geocentric radial distance of 1.47 Re, 400 kHz at 1.58 Re, 300 kHz at 1.74 Re, 200 kHz at 1.98 Re, 100 kHz at 2.47 Re, 50 kHz at 3.09 Re, 30 kHz at 3.60 Re, and 15 kHz at 4.52 Re. Subtracting 1 Re yields the altitude. In the duskside plasmasphere, the electron density is enhanced so that the density in the auroral plasma cavity should be hard to decrease enough to satisfy the condition for the electron cyclotron maser instability. Therefore, generation of high-frequency AKR at lower altitudes is expected to be blocked on the duskside hemisphere.

Kasaba et al. (1997) found that at both 200 kHz and 500 kHz the frequency of occurrence of AKR was positively correlated with the Kp index and that this was more evident for the 200 kHz data. The latter agreed with an earlier finding of Kaiser and Alexander (1977a) that the frequency of the peak flux of AKR was inversely correlated with the AE index. These results indicate that the AKR source region moves up in altitude under disturbed geomagnetic conditions. Kasaba et al. (1997) also found that the illumination region increased in size during active times with an equatorward extension common at both frequencies which is believed to be due to the equatorward shift of the auroral plasma cavity in the disturbed phase expected from the inward motion of the plasmapause just after the onset of substorms. For the duskside region and at higher magnetic latitudes, the illumination pattern became larger for 200 kHz than for 500 kHz as the geomagnetic activity increased. This was believed to be due to the influence of the evening plasmaspheric bulge on the AKR propagation especially at the lower altitudes. Another important new result from Kasaba et al. (1997) was that AKR is more active on the winter hemisphere especially for the high frequency range. Possible reasons include asymmetry of the population of precipitating electrons on the auroral field lines and insufficient density depression in the auroral plasma cavity on the summer hemisphere especially at lower altitudes which are most sensitive to ionospheric outflow.

Terrestrial low frequency (LF) bursts are a part of AKR often observed during geomagnetic storms and strong substorms (Steinberg et al., 1988, 1990, 1998; Kaiser et al., 1996; Anderson et al., 1997, 1998, 2001). Frequently the LF bursts occur during a period of the lower cutoff frequency of AKR continually decreasing. Alexander and Kaiser (1976) first reported that the AKR lower cutoff frequency tended to move to lower frequencies during geomagnetically disturbed periods. Frequently the upper frequency limit increases indicating that the source region is then also expanding to lower altitudes. The changing upper and lower frequency limits observed during substorms can be used to study the dynamics of the plasma in the AKR source region. The POLAR WBR has yielded exciting data on the fine structure of AKR as well as details on the structure of LF bursts. Data from the plasma wave instruments on GEOTAIL and POLAR and the radio science experiment on WIND will be used here to study the characteristics and relationship of AKR and LF bursts. These three spacecraft and the CANOPUS (Rostoker et al., 1995) ground magnetometer network which provided data for this study were all parts of the ISTP/GGS program. We will concentrate first on quasi-periodic AKR low frequency enhancements well correlated with ground magnetometer observations and then on multi- spacecraft observations of the enhanced AKR resulting in LF burst observations in the magnetosphere and in the solar wind. We will examine events that illustrate the nature of AKR and LF bursts and their relationships to other measures of geomagnetic activity and we will compare simultaneous observations from different regions of space.

OBSERVATIONS

Quasi-periodic Intensifications

An interesting characteristic of many of the LF bursts that we have observed is that they occur as a part of a series of quasi-periodic AKR bursts whose lower cutoff frequencies progressively decrease. After the LF burst occurs, a series of quasi-periodic AKR bursts whose lower cutoff frequencies increase progressively to higher frequencies often follows. An example of this is shown in Figure 1 which displays the GEOTAIL PWI

Sweep Frequency Analyzer (SFA) data on February 23, 1994, from 03:00 UT to 05:00 UT. GEOTAIL was about 85 Re behind and towards the dusk side of the Earth in the solar wind just outside the early evening magnetosheath at GSE (X, Y, Z) = (-47.7 Re, 69.5 Re, -4.6 Re) and GSM (X, Y, Z) = (-47.7 Re, 64.1 Re, 27.4 Re). WIND and POLAR had not yet been launched. Five distinct events occur between 03:30 UT and 04:45 UT in which the AKR intensifies and its lower frequency cutoff progressively decreases (until 04:00 UT) and then increases (after 04:05 UT). The decreasing lower cutoff frequency means that the conditions required for the generation of AKR are moving to higher altitudes. These conditions include the local Fp in the source region being significantly less than the local Fce and that there be a source of free energy from a positive slope in the perpendicular electron velocity distribution.

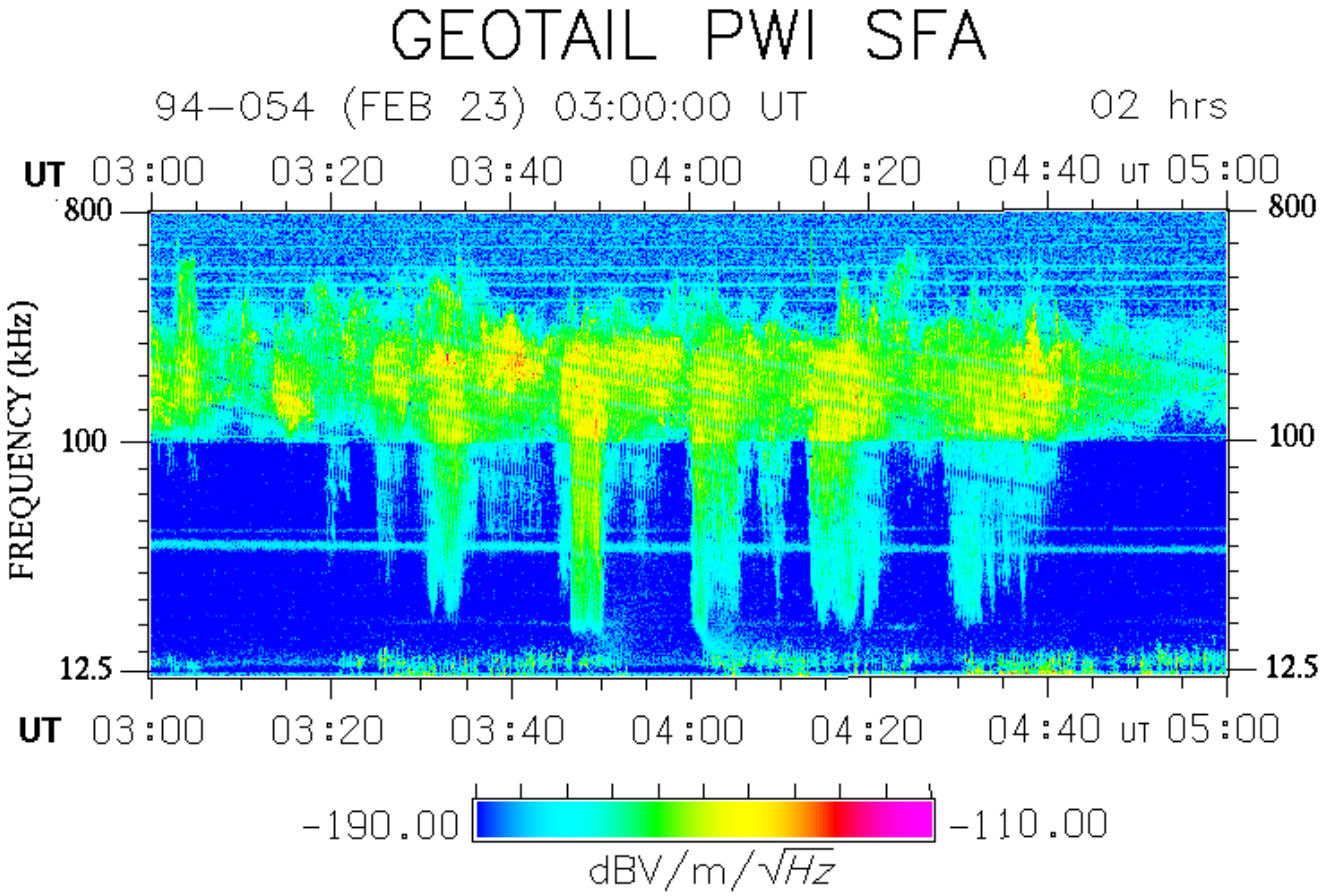

Fig. 1. The GEOTAIL PWI electric field SFA data for 03:00 UT to 05:00 UT on February 23, 1994. The data shown are on linear frequency scales from 12.5 kHz to 100 kHz and from 100 kHz to 800 kHz. Five distinct quasi-perioidic enhancements in the AKR are evident between 03:30 UT and 04:45 UT that include the lower frequency cutoff significantly decreasing until 04:00 UT and then increasing after 04:05 UT. These enhancements are coincident with negative bay onsets and Pi2 oscillations shown in Figure 2. The diffuse tail of a terrestrial LF burst is evident beginning near 30 kHz at 04:00 UT which reaches 15 kHz before 04:05 UT.

The nearly-constant-frequency emission line near 15 kHz is at the local electron plasma frequency Fp. The frequent enhancements in intensity are Langmuir waves excited when the region is magnetically connected to the Earth's bow shock (Kasaba et al., 2000). The weak narrow emission line just above 30 kHz is the 2Fp line which is generated near the Earth's bow shock on or just downstream of magnetic field lines tangent to the Earth's bow shock (Reiner et al., 1996) The plasma frequency in the near-Earth magnetosheath is 2Fp at the bow shock and gradually decreases downstream until it equals the local solar wind Fp. A LF burst is evident beginning near 30 kHz at 04:00 UT which reaches 15 kHz before 04:05 UT. The LF burst after falling below the 2Fp line approaches the Fp line with increasingly longer delay times. This long diffuse tail is an identifiable characteristic of the LF bursts. A very weak LF burst also is detected between 30 kHz and 15 kHz beginning at 03:48 UT and lasting for about five minutes.

Table 1. CANOPUS Magnetometer Sites

		Geodedic		Pace			Inv.
Location	Acronym	Lat.	Long.	Lat.	Long.	L	Lat.
Rankin Inlet	RANK	62.8	267.9	73.7	-29.0	12.4	73.5
Eskimo Point	ESKI	61.1	266.0	71.9	-31.8	10.2	71.7
Fort Churchill	FCHU	58.8	265.9	69.7	-30.8	8.2	69.6
Gillam	GILL	56.4	265.4	67.4	-30.9	6.7	67.3
Island Lake	ISLL	53.9	265.3	64.9	-30.3	5.5	64.8
Pinawa	PINA	50.2	264.0	61.2	-31.6	4.3	61.2
Rabbit Lake	RABB	58.2	256.3	67.8	-45.0	6.9	67.6
Contwoyto Lake	CONT	65.8	248.8	73.4	-61.2	12.4	73.5
Fort Smith	FSMI	60.0	248.1	67.9	-57.3	7.1	68.0
Fort McMurray	MCMU	56.7	248.8	64.8	-54.4	5.5	64.8
Fort Simpson	FSIM	61.7	238.8	67.6	-69.9	6.8	67.4
Dawson	DAWS	64.1	220.9	65.9	-90.1	5.9	65.7

The geomagnetic conditions were moderately active with Kp = 3+ and DST = -57 nT. Slightly more than one day earlier a strong storm produced Kp = 8- and DST = -144 nT. The north-south (X) components of the CANOPUS array ground magnetometer data for 0300 UT to 0500 UT on February 23, 1994, are shown in Figure 2. The locations of the twelve stations for which there are data are listed in Table 1.

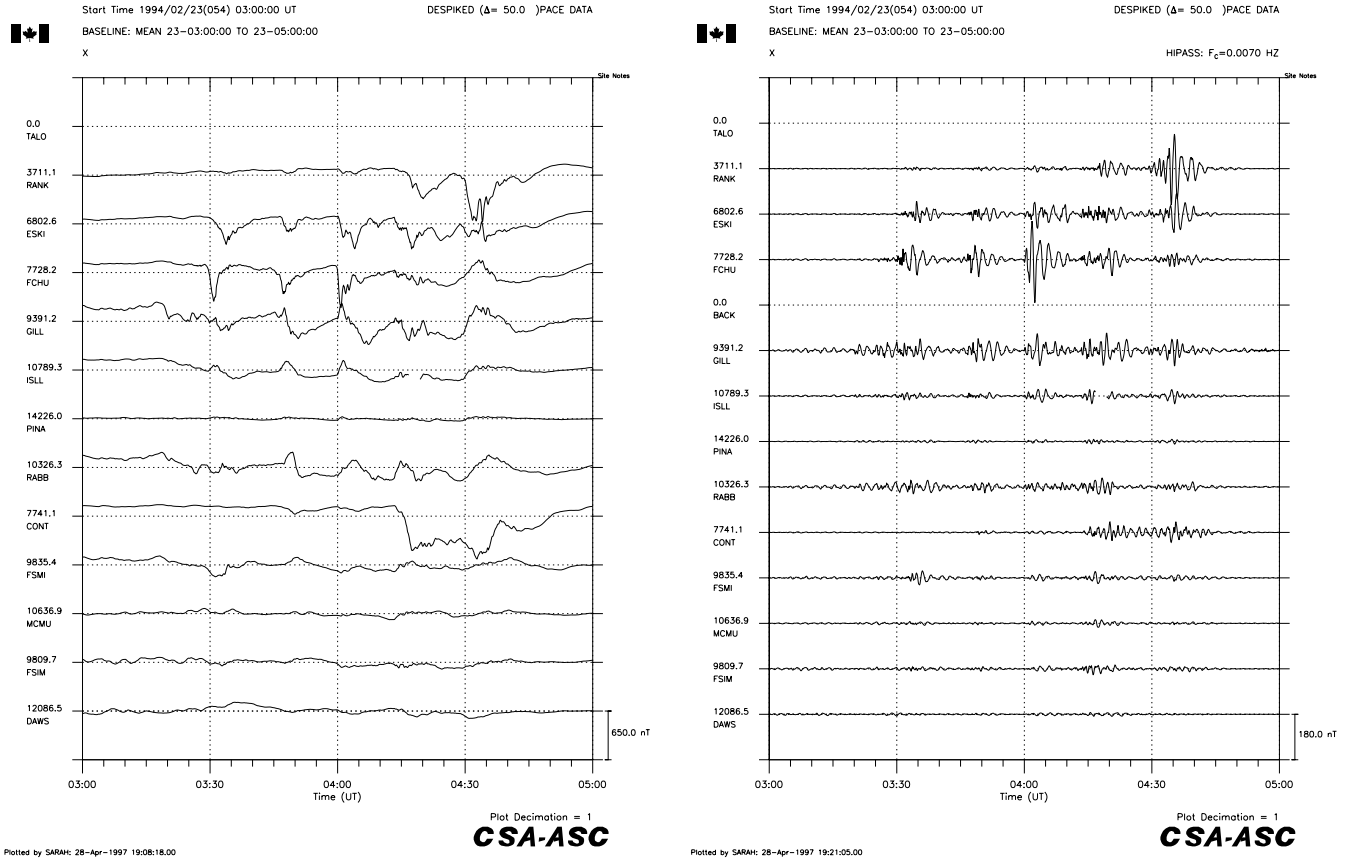

Fig. 2. The CANOPUS array magnetometer north-south (X) component data for 03:00 UT to 05:00 UT on February 23, 1994. Panel A, the left panel, is unfiltered and Panel B, the right panel, is high-pass filtered with fc = 7 mHz which highlights Pi2 oscillations associated with expansive phase onsets. Full scale in Panel A is 650 nT and full scale in Panel B is 180 nT. The quasi-periodic negative bay onsets and Pi2 oscillation enhancements correspond well with the five AKR LF enhancements in Figure 1.

Strong negative bays of the order of several hundred nT and strong Pi2 oscillations are evident especially in the Fort Churchill and Eskimo Point data for the first three distinct events and also in the higher latitude Rankin Inlet data for the final two. Both are indicative of expansive phase onsets. The LF burst beginning at 04:00 UT and the AKR lower cutoff frequency reaching its lowest value are coincident with the strongest Pi2 oscillation observed for the two-hour period.

The solar wind speed measured by the GEOTAIL Comprehensive Plasma Instrument (CPI) (Frank et al., 1994) was high at about 700 km/sec (K. L. Ackerson, Private Communication). Desch et al. (1996) and Desch (1997) found that the occurrence of LF bursts were well correlated with the solar wind speed and somewhat less correlated with the azimuthal direction of the IMF. The LF bursts tended to occur in the sectors when the IMF was pointed towards the sun. They concluded that the LF bursts were a signature of a large-scale process of magnetospheric energy dissipation. They suggested a viscous-like interaction between the solar wind and the magnetosphere. For this event, the solar wind speed was higher than normal but the measurements were made in an away sector.

AKR generated in the auroral region above twice the solar wind plasma frequency can propagate directly through the magnetosheath into the solar wind. The diffuse tails of the LF bursts are believed to be due to the lowest frequency portion of the AKR waves scattering far down the tail where the plasma frequency of the magnetosheath reaches the solar wind plasma frequency. Nearer the Earth these waves are reflected by the high density encountered at the magnetopause. As an electromagnetic wave approaches a region where the plasma frequency is near the wave frequency, the group velocity decreases and the delay time increases. The closer the frequency of the wave is to the plasma frequency, the slower it travels and the more likely it is to be scattered. As the magnetosheath density decreases further down the tail, it approaches the solar wind density. The scattering can thus carry the waves out into the solar wind. This results in a very large apparent source size for the radiation which would have no spin modulation.

Multi-Spacecraft Observations

On January 28, 1997, the WIND spacecraft was 174 Re upstream of the Earth near the Earth-Sun line at GSE X = 172 Re, GSE Y = -20 Re, and GSE Z = -16 Re.

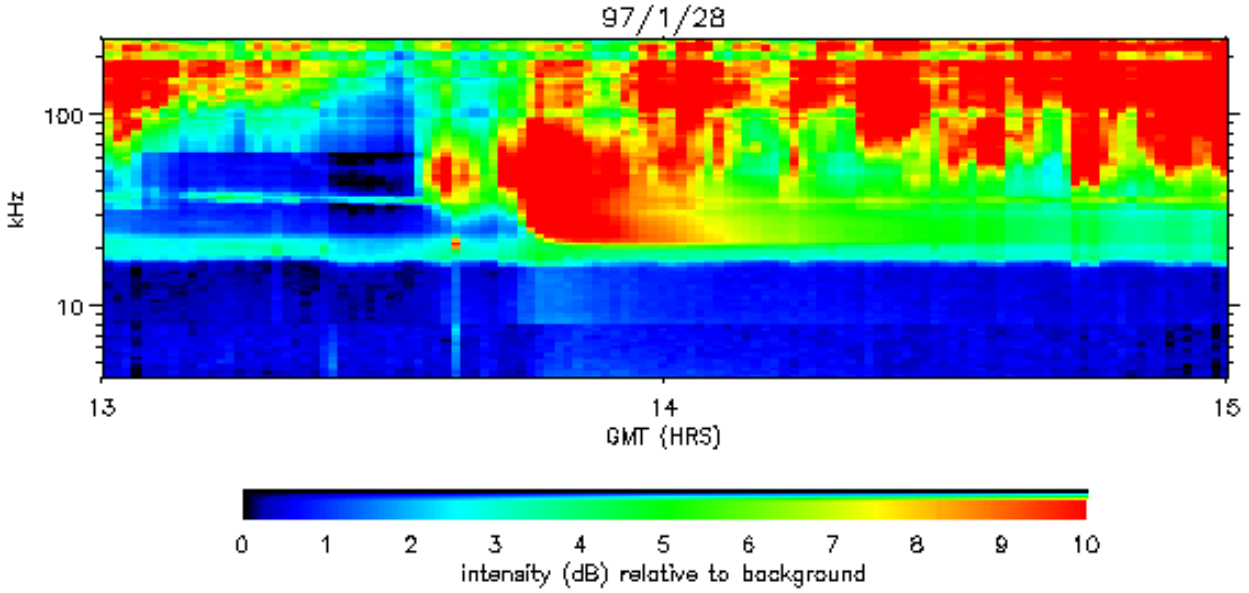

Fig. 3. The WIND/WAVES TNR data for 13:00 UT to 15:00 UT on January 28, 1997 when WIND was 174 Re upstream of the Earth. The data shown are on a logarithmic frequency scale from 4 kHz to 256 kHz. The color-coded intensity scale covers 10 dB relative to the receiver background. The LF burst beginning at 13:42 UT has a distinctive diffuse tail.

The solar wind speed (from the WIND comprehensive plasma experiment SWE (Ogilvie et al., 1995)) was high at about 650 km/s such that the local solar wind parameters would reach Earth in about 28 minutes.

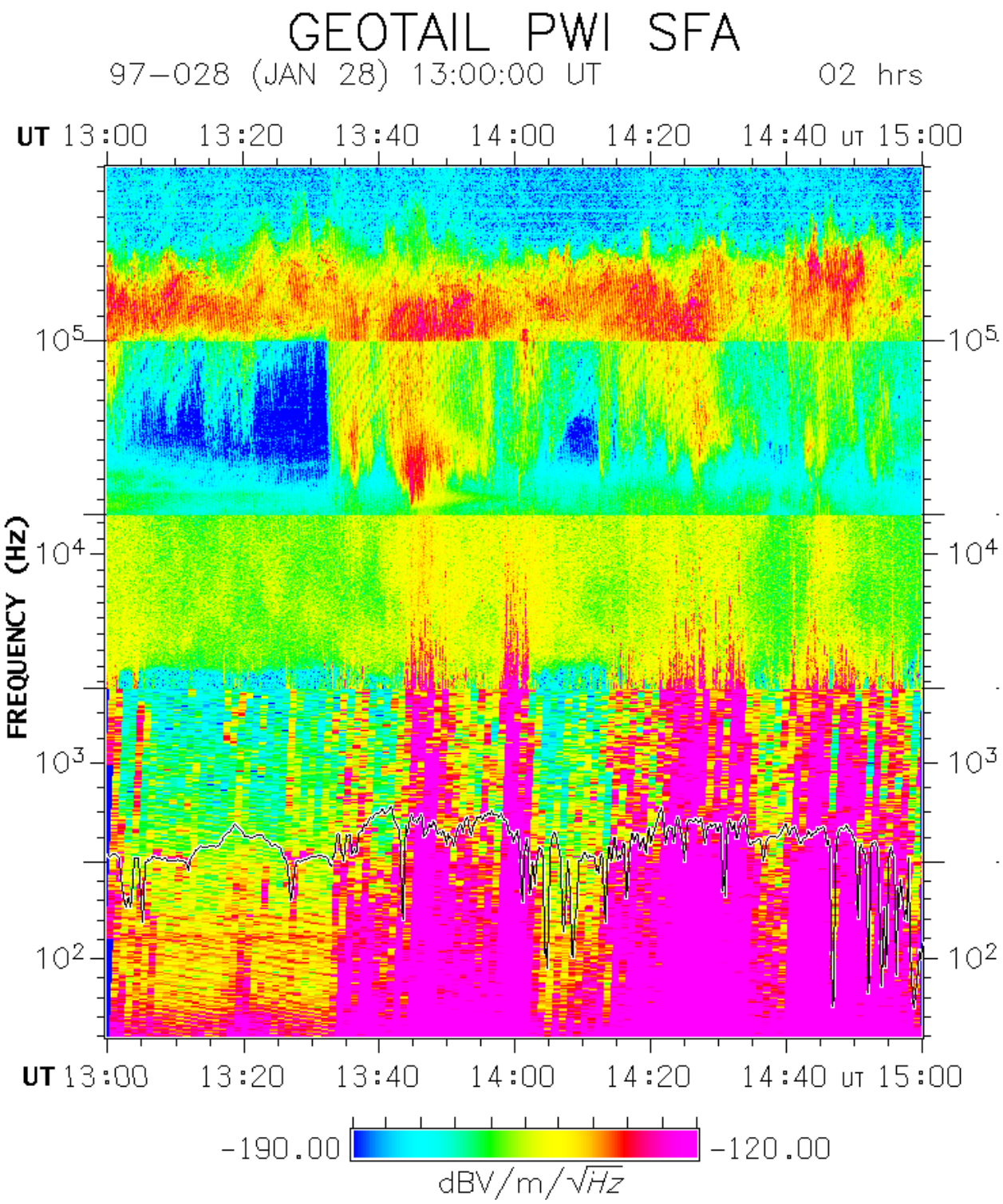

Fig. 4. The GEOTAIL PWI electric field SFA data for 13:00 UT to 15:00 UT on January 28, 1997 when GEOTAIL was about 30 Re down the tail. The data are displayed in five linear frequency bands: 25 Hz to 200 Hz, 200 Hz to 1600 Hz, 1.6 kHz to 12.5 kHz, 12.5 kHz to 100 kHz, and 100 kHz to 800 kHz. The intensity is color coded over a 70 dB dynamic range. The black and white line near the bottom of the spectrogram indicates the local electron cyclotron frequency determined from the GEOTAIL MGF experiment. Just before 13:40 UT the lower cutoff frequency of the AKR began to fall and reached below 20 kHz at 13:44 UT. A tapered diffuse tail centered very near 20 kHz is evident for about ten minutes after 13:44 UT.

Two LF bursts that were detected at WIND in the second half of the day will be examined here to better understand their relationship to the AKR observed. One began at 13:42 UT and the second began around 19:05 UT. Geomagnetic activity was moderately active with with Kp from 12 UT to 21 UT being 4, 4, and 4+. Figure 3 shows the WIND/WAVES TNR spectrogram for the 4 kHz to 256 kHz logarithmic frequency range from 13:00 UT to 15:00 UT. The intensity is color coded over a 10 dB range relative to the receiver background. The emission line near 20 kHz at the beginning of the plot is at the local electron plasma frequency Fp. The narrow emission line near 40 kHz at the beginning of the plot and which decreases to about 35 kHz by the end of the plot is the 2Fp line which is generated near the Earth's bow shock. The LF burst began between 40 and 70 kHz in frequency at 13:42 UT and fell below the 2Fp line at 13:44 UT and then approached the Fp line with increasingly longer delay times. The other emissions above 2Fp are AKR.

The GEOTAIL and POLAR PWI data for the same two-hour period are shown in Figures 4 and 5, respectively. GEOTAIL was about 30 Re down the tail at GSE X = -28.3 Re, GSE Y = 10.2 Re, and GSE Z = -3.2 Re and was moving toward the center of the tail. The 2 kHz lower cutoff of the continuum radiation (which here extends from 2kHz to 12 kHz) is at the local plasma frequency and indicates low number densities around 0.04 e/cc. Several times throughout this period the lower cutoff frequency of the AKR fell below 100 kHz.

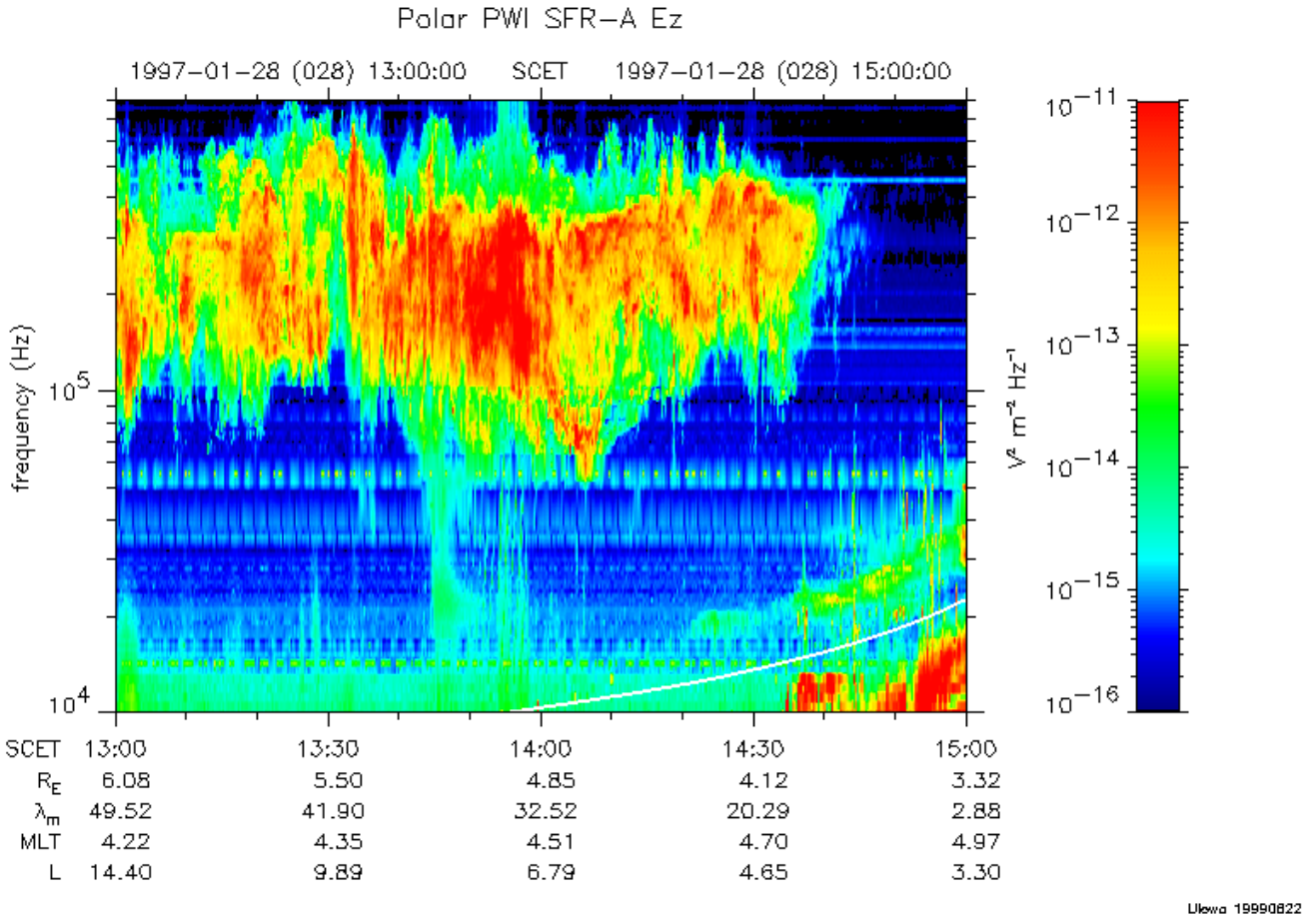

Fig. 5. The POLAR PWI SFR Ez data for 13:00 UT to 15:00 UT on January 28, 1997 when POLAR was in the pre-dawn sector (4.5 MLT) approaching the plasmasphere. The data shown are on a logarithmic frequency scale from 10 kHz to 800 kHz. The intensity is color coded over a 50 dB dynamic range. The white line which crosses 10 kHz just before 14:00 UT is the electron cyclotron frequency determined from the ambient magnetic field measurements of the POLAR MFI experiment (Russell et al., 1995). The LF burst with the tapered tail centered on 20 Khz is clearly evident beginning at 13:44 UT.

In the period from 13:30 UT to 15:00 UT we see that when the AKR emissions appeared below 100 kHz that the AKR above 100 kHz was enhanced and that strong extremely low frequency (ELF) emissions (from 25 Hz to 1-3 kHz) occurred simultaneously. These elf emissions accompany the bursty bulk flows that have been identified with substorms and AKR intensifications (Fairfield et al., 1998,1999). However, only one of these episodes produced a clear LF burst that was also detected by WIND. Just before 13:40 UT the lower cutoff frequency of the AKR began to fall and reached below 20 kHz at 13:44 UT. A tapered diffuse tail centered very near 20 kHz is evident for about ten minutes after 13:44 UT. Only when the AKR reaches a frequency significantly below the maximum magnetosheath frequency (twice the solar wind plasma frequency at the bow shock) is a LF burst observed.

Figure 5 displays the POLAR PWI SFR Ez (the electric field measured by the antenna along the spacecraft spin-axis) data logarithmically from 10 kHz to 800 kHz. The LF burst with the tapered tail centered on 20 Khz is clearly evident beginning at 13:44 UT. Note that the strong AKR observed on GEOTAIL after 14:40 UT is not present in the POLAR data. It has been refracted away by the dense plasmasphere.

The WIND/WAVES TNR data from 18:00 UT to 20:00 UT over a 12 dB range relative to the receiver background are shown in Figure 6. The LF burst begins above 256 kHz and falls below the 2Fp line at 19:05 UT and approaches the Fp line with increasingly longer delay times. Fp and 2Fp have fallen slightly from five hours earlier to 18 kHz and 36 kHz, respectively. The GEOTAIL PWI SFA data over a 70 dB dynamic range for the same two-hour time period are shown in Figure 7. A LF burst with a tapered tail centered on 20 Khz is clearly evident from about 19:05 UT to 19:15 UT. Note that the strong ELF waves believed to be associated with bursty bulk flows occur from 18:50 UT to 19:13 UT simultaneously with the lower cutoff frequency of AKR being very low. The POLAR PWI SFR Ez data are shown in Figure 8. Polar near dusk (18 MLT) has exited the plasmasphere and is headed for its north pole apogee. Diffuse emissions down to about 15 kHz are present from 19:05 UT to 19:15 UT. Very intense AKR reaches as low as 32 kHz at about 19:13 UT.

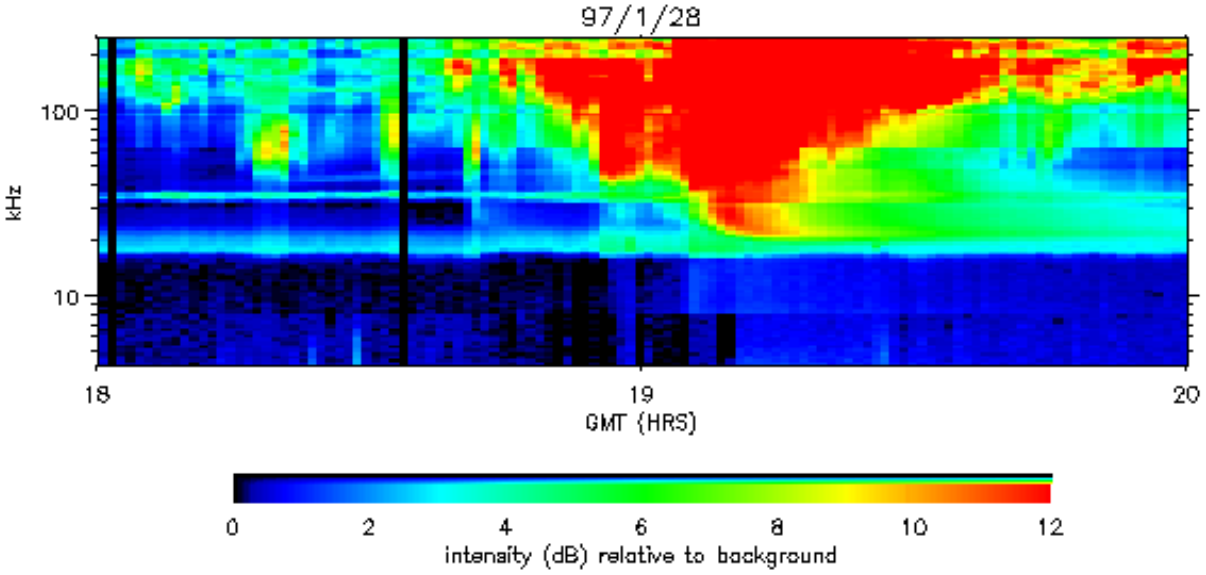

Fig. 6. The WIND/WAVES TNR data for 18:00 UT to 20:00 UT on January 28, 1997. The color-coded intensity scale covers 12 dB relative to the receiver background. The LF burst beginning at 19:05 UT has a distinctive diffuse tail.

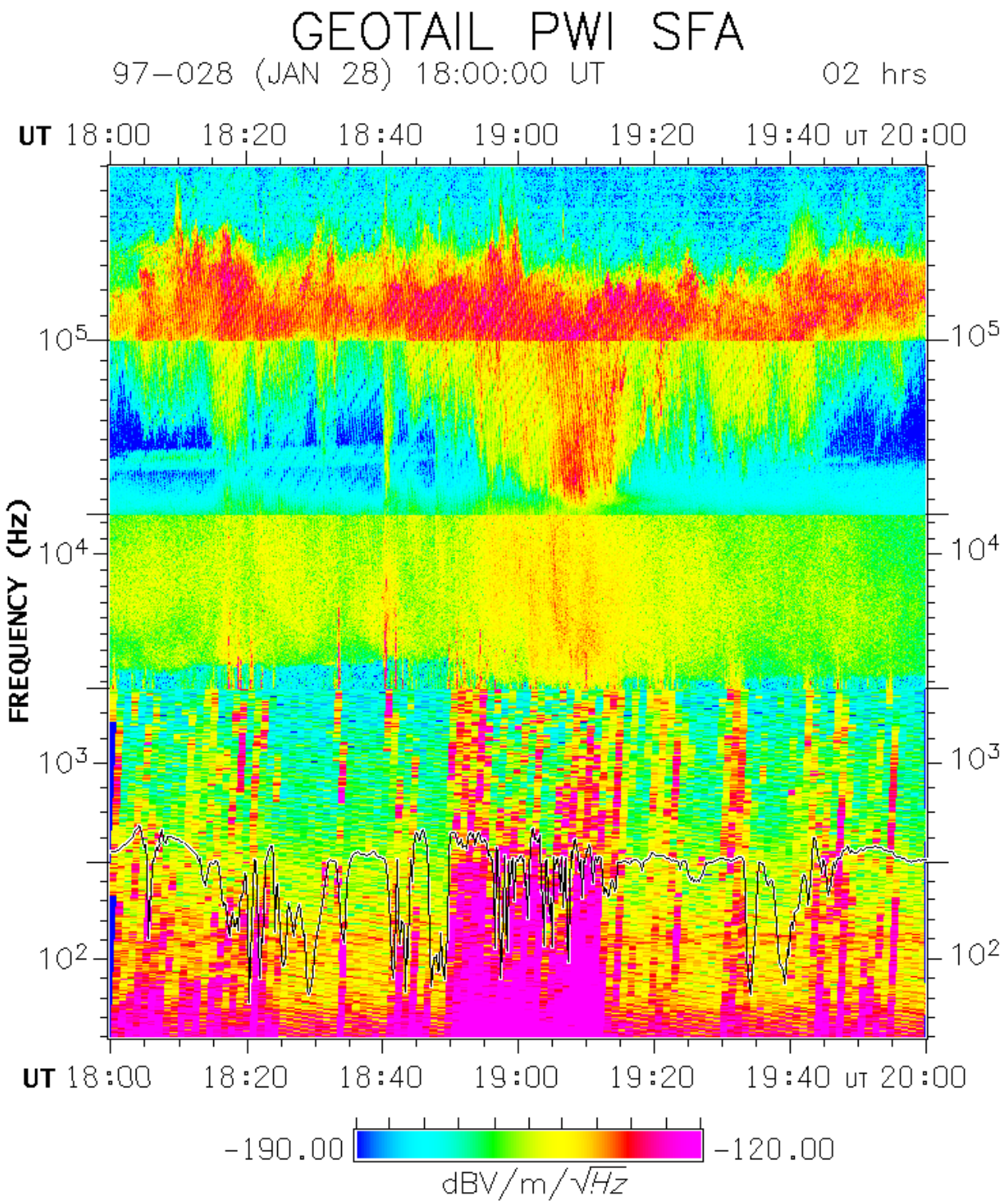

Fig. 7. The GEOTAIL PWI SFA data for 18:00 UT to 20:00 UT on January 28, 1997. A LF burst with a tapered tail centered on 20 Khz is clearly evident from about 19:05 UT to 19:15 UT. Strong ELF waves associated with bursty bulk flows occur from 18:50 UT to 19:13 UT simultaneously with the lower cutoff frequency of AKR being very low.

POLAR PWI WBR data in the 0-90 kHz mode were available for the 19:05 UT LF burst and showed that there was a distinct difference in the higher frequency AKR in this case as compared to the lower frequency AKR. The higher frequency AKR was more intense and the discrete structure was spin modulated and at least initially was predominantly rising in frequency. In the lower frequency portion the discrete emissions

were dominated by falling frequency stripe-like features that were not always well spin-modulated. Near the end of the WBR data after about 19:11 UT the lower cutoff frequency of the more intense higher frequency AKR dropped to about 32 kHz and the weaker lower frequency portion extended below 20 kHz. What we have seen here is that POLAR does observe AKR that is detected as a LF burst by GEOTAIL and WIND but that the lowest frequency portion is less intense and has different discrete structure. One possibility is that a more intense lower frequency portion is generated near or earlier than local midnight that is more visible to GEOTAIL situated close to local midnight.

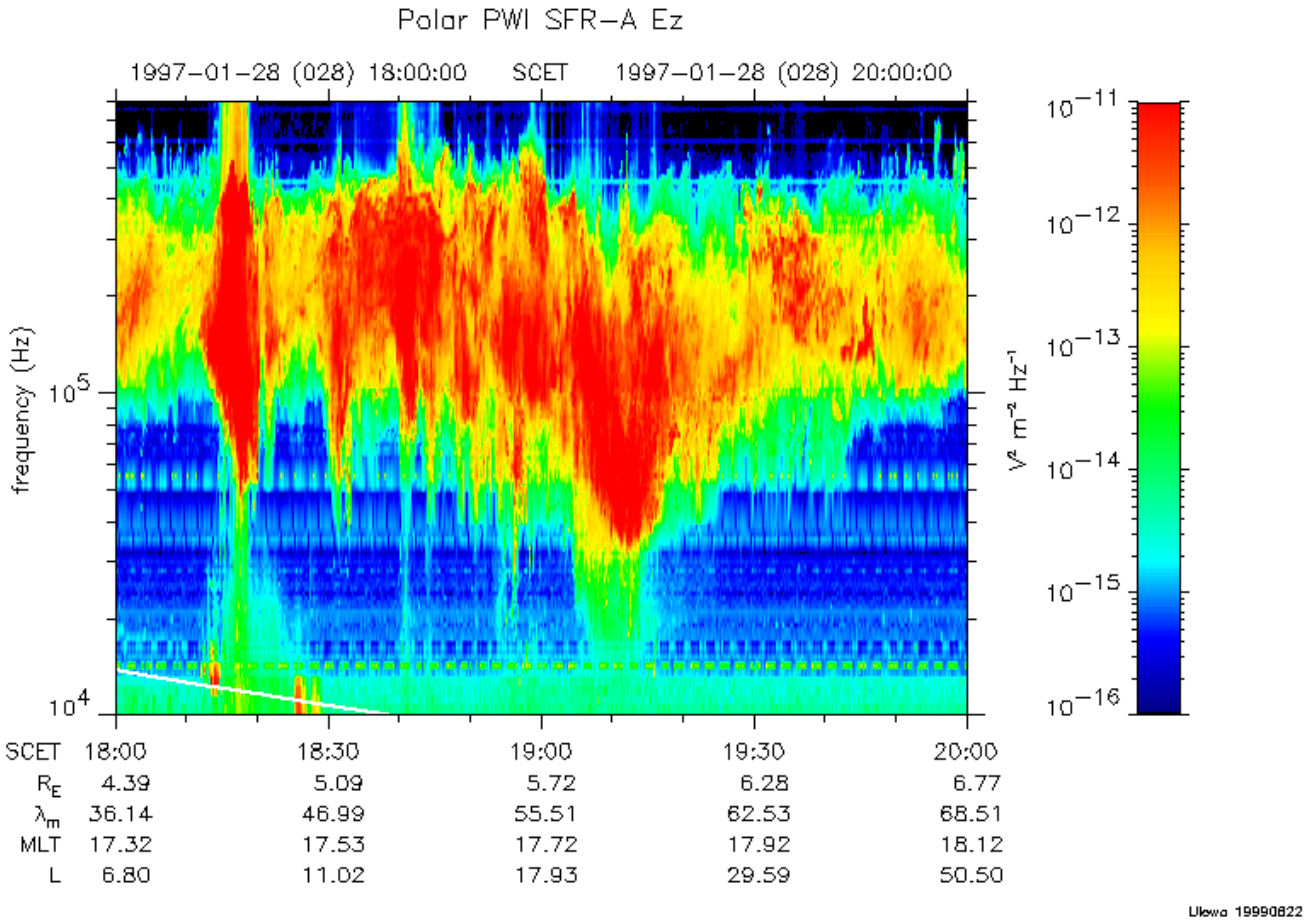

Fig. 8. The POLAR PWI SFR Ez data for 18:00 UT to 20:00 UT on January 28, 1997. POLAR was near dusk (18 MLT), had exited the plasmasphere, and was headed for its north pole apogee. Diffuse emissions down to about 15 kHz are present from 19:05 UT to 19:15 UT. Very intense AKR reaches as low as 32 kHz at about 19:13 UT.

DISCUSSION AND SUMMARY

GEOTAIL and POLAR PWI measurements along with those from the WIND WAVES experiment, the CANOPUS ground optical data and magnetograms, the IMAGE Network magnetograms, and POLAR auroral imaging have provided new information on AKR and LF bursts and their relationships to the magnetospheric plasma dynamics. AKR measurements when a satellite can view the nightside hemisphere provide excellent indications of substorm onsets. The absence of higher frequency AKR in some upstream observations of LF bursts can be attributed to propagation blockage by the Earth and dense plasmasphere of the portion of the AKR generated at the lowest altitudes on the night side. The ideal situation for substorm onset identification would include the simultaneous availability of multiple spacecraft observations of AKR covering all local times, worldwide ground all sky camera, magnetometer, and meridian scanning

photometer measurements, and space-based auroral imaging. The combination of the high time-resolution and remote sensing capabilities provided by the plasma wave measurements make them very important for studying the triggering, near triggering, and burstiness of substorms and related geomagnetic disturbances.

We have found that LF bursts are the lower frequency portion of AKR and are produced simultaneously with intense isolated substorms. Spacecraft observations often show that the AKR increases in intensity and its lower frequency limits decrease when LF bursts are observed indicating that the AKR source region is expanding to higher altitudes. Since AKR is generated near the local electron cyclotron frequency, the frequency of AKR identifies the location along a magnetic field line where it is generated and the lower the frequency, the higher the altitude. This relationship allows us to investigate some source characteristics such as the average speed for the upward movement of the AKR source region. Frequently the upper frequency limit also increases indicating that the source region is then also expanding to lower altitudes. In the future we will examine source speeds for all the LF events with measurable upper and lower cutoff frequencies. We will look for geophysical parameters that might correlate with the speeds.

In a limited number of cases that we have been able to examine in detail, CANOPUS ground magnetometer and meridian scanning photometer data show that during the LF burst events the expansive phase onsets start at unusually low latitudes and move poleward and westward. The data also show that the LF bursts occur when the expansive phase onset signatures are most intense. Many of the LF bursts occurred related to CME events observed by SOHO which were identified by the NOAA SEC as being highly geoeffective. Magnetometer data from geosynchronous satellites usually show increased magnetic field dipolarization and the presence of field-aligned currents during LF burst events. Large injections of protons and electrons have also been detected by the GOES and LANL geosynchronous satellites during LF burst events. AKR-produced low frequency bursts which occur during the more intense geomagnetic disturbances thus provide a space weather marker of the geoeffectiveness of the events. We will continue to investigate the global activity that is associated with and leads to LF bursts. The already productive correlative studies with the POLAR x-ray and optical imaging are continuing and will now concentrate on LF burst events.

We will also continue the investigation of the dimensions and shape of the geomagnetic tail. Our analysis using our tapered-tail LF burst observations and solar wind speed and density measurements from available spacecraft have yielded tail lengths fron 200 Re to over 2000 Re. Desch (1997) calculated travel times for LF burst emissions and found that observations required the emissions having had to travel as much as 2000 Re down the tail. Steinberg et al. (1998) used WAVES direction finding measurements to find that the spin-modulated high frequency portion of LF bursts exited the bow shock from 100 Re to 460 Re down the tail. Desch and Farrell (2000) studied a LF burst that was occulted by a strong increase of solar wind plasma density 97 Re down the tail. Thus the LF burst had to have entered the solar wind beyond 97 Re down the tail. Steinberg et al. (2003) analyzed 119 LF bursts observed by WIND WAVES when the spacecraft was near the Lagrange Point L1 and concluded that the bow shock still exists beyond 1000 Re.

A topic for future study is determining what solar wind parameters control the length of the Earth's geomagnetic tail. Another worthwhile topic to be pursued is trying to determine the reasons for the quasi-periodic nature of many geomagnetic disturbances and whether or not they contradict the importance of self organized criticality in magnetospheric dynamics. We have well demonstrated in this paper that GEOTAIL, POLAR, and WIND are still valuable resources for the study of the Earth's magnetosphere and the heliosphere.

ACKNOWLEDGMENTS

We thank all members of the ISTP team for the high quality data and for the successful spacecraft operation. R. R. Anderson appreciates support for his participation in this research under his Visiting Professorship at RASC, Kyoto University, and at The University of Iowa by NASA Contract NAS5-30371 and NASA Grants NAG5-2346, NAG5-7110, NAG5-7943, and NAG5-11707, all with Goddard Space Flight Center. Portions of this research were supported by Grant-in-Aid for Scientific Research (A) 12304026 from Japan Society for the Promotion of Science (JSPS).

REFERENCES

Acuna, M. H., K. W. Ogilvie, D. N. Baker, S. A. Curtis, D. H. Fairfield, and W. H. Mish, The Global Geospace Science Program and its investigations, Space Sci. Rev., 71, 5-21, 1995.

Alexander, J. K., and M. L. Kaiser, Terrestrial Kilometric Radiation 1. Spatial Structure Studies, J. Geophys. Res., 81, 5948, 1976]

Anderson, R. R., D. A. Gurnett, H. Matsumoto, K. Hashimoto, H. Kojima, Y. Kasaba, M. L. Kaiser, G. Rostoker, J.-L. Bougeret, J.-L. Steinberg, I. Nagano, and H. Singer, Observations of low frequency terrestrial type III bursts by GEOTAIL and WIND and their association with isolated geomagnetic disturbances detected by ground and space-borne instruments, Planetary Radio Emissions IV, Proc. Graz Conf., ed. by H. O. Rucker, S. J. Bauer, and A. Lecacheux, Austrian Academy of Sciences Press, Vienna, 241-250, 1997.

Anderson, R. R., D. A. Gurnett, L. A. Frank, J. B. Sigwarth, H. Matsumoto, K. Hashimoto, H. Kojima, Y. Kasaba, M. L. Kaiser, G. Rostoker, J.-L. Bougeret, J.-L. Steinberg, I. Nagano, T. Murata, H. J. Singer, T. G. Onsager, and M. F. Thomsen, Geotail, Polar, Wind, CANOPUS, and ISTP associated geosynchronous satellite observations of plasma wave emissions and related magnetospheric phenomena during substorms, in Proceedings of International Conf. on Substorms-4, ISC-4, edited by S. Kokubun and Y. Kamide, pp. 567-572, Kluwer Academic Publishers, Dordrecht, London, Boston, and Terra Scientific Publishing Company, Tokyo, 1998.

Anderson, R. R., H. Matsumoto, K. Hashimoto, H. Kojima, I. Nagano, Y. Kasaba, M. L. Kaiser, J.-L. Bougeret, and J. L. Steinberg, Using Geotail, Wind, and Polar observations of solar, interplanetary, and terrestrial plasma wave and radio emissions to identify source characteristics, in Planetary Radio Emissions V, ed. H. O. Rucker, M. L. Kaiser, and Y. Leblanc, pp. 297-310, 2001.

Bougeret, J.-L., M. L. Kaiser, P. J. Kellogg, R. Manning, K. Goetz, S. J. Monson, N. Monge, L. Friel, C. A. Meetre, C. Perche, L. Sitruk, and S. Hoang, WAVES: The radio and plasma wave investigation on the WIND spacecraft, Space Sci. Rev., 71, 231-263, 1995.

Desch, M. D., Terrestrial LF Bursts: Source and solar wind connection, in *Planetary Radio Emissions IV, Proc. Graz Conf.*, ed. by H. O. Rucker, S. J. Bauer, and A. Lecacheux, Austrian Academy of Sciences Press, Vienna, 251-258, 1997.

Desch, M. D., and W. M. Farrell, Terrestrial LF Bursts: Escape paths and Wave Intensification, in *Radio Astronomy at Long Wavelengths*, **AGU Geophysical Monograph 119**, R. G. Stone, K. W. Weiler, M. L. Goldstein, and J.-L. Bougeret, editors, pp. 205-211, 2000.

Desch, M. D., M. L. Kaiser, and W. M. Farrell, Control of terrestrial low frequency bursts by solar wind speed, Geophys. Res. Lett., 23, 1251-1254, 1996.

Ergun. R. E., C. W. Carlson, J.P. McFadden, F. S. Mozer, G. T. Delory, W. Peria, C. Chaston, M. Temerin, R. Elphic, R. Strangeway, R. Pfaff, C. A. Cattell, D. Klumpar, E. Shelly, W. Peterson, E. Moebius, and L. Kistler, FAST satellite wave observations in the AKR source region, Geophys. Res. Lett., 25, 2061, 1998.

Fairfield, D. H., T. Mukai, A. T. Y. Lui, C. A. Cattell, G. D. Reeves, T. Nagai, G. Rostoker, H. J. Singer, M L. Kaiser, S. Kokubun, A. J. Lazarus, R. P. Lepping, M. Nakamura, J. T. Steinberg, K. Tsurda, D. J. Williams, and T. Yamamoto, Geotail observations of substorm onset in the inner magnetotail, J. Geophys. Res., 103, 103-117, 1998.

Fairfield, D. H., T. Mukai, M. Brittnacher, G. D. Reeves, S. Kokubun, G. K. Parks, T. Nagai, H. Matsumoto, K. Hashimoto, D. A. Gurnett, and T. Yamamoto, Earthward flow bursts in the inner magnetotail and their relation to auroral brightenings, AKR intensifications, geosynchronous particle injections and magnetic activity, J. Geophys. Res., 104, 355-370, 1999.

Frank, L. A., K. L. Ackerson, W. R. Paterson, J. A. Lee, M. R. English, and G. L. Pickett, Comprehensive plasma instrumentation (CPI) for the GEOTAIL spacecraft, J. Geomag. Geoelectr., 46, 23-37, 1994.

Green, J. L., D. A. Gurnett, and S. D. Shawhan, The angular distribution of auroral kilometric radiation, J. Geophys. Res., 82, 1825, 1977.

Green, J. L., and D. L. Gallagher, The detailed intensity distribution of the AKR emission cone, J. Geophys. Res., 90, 9641, 1985.

Gurnett, D. A., The earth as a radio source: Terrestrial kilometric radiation, J. Geophys. Res., 79, 4227, 1974.

Gurnett, D. A., A. M. Persoon, R. F. Randall, D. L. Odem, S. L. Remington, T. F. Averkamp, M. M. DeBower, G. B. Hospodarsky, R. L. Huff, D. L. Kirchner, M. A. Mitchell, B. T. Pham, J. R. Phillips, W. J. Schintler, P. Sheyko, and D. R. Tomash, The POLAR plasma wave instrument, Space Sci. Rev., 71, 597-622, 1995.

Hashimoto, K., H. Matsumoto, T. Murata, M. L. Kaiser, and J.-L. Bougeret, Comparison of AKR simultaneously observed by the GEOTAIL and WIND spacecraft, Geophys. Res. Lett., 853-856, 1998.

Imhof, W.L., K.A. Spear, J.W. Hamilton, B.R. Higgins, M.J. Murphy, J.G. Pronko, R.R. Vondrak, D.L. McKenzie, C.J. Rice, D. J. Gorney, D.A. Roux, R.L. Williams, J A. Stein, J. Bjordal, J. Stadsnes, K. Njoten, T.J. Rosenberg, L. Lutz, D. Detrick, The Polar Ionospheric X-ray Imaging Experiment, (Reprinted in The Global Geospace Mission, ed. by C.T. Russell, Kluwer Academic Publishers,1995), Space Science Reviews, 71, Nos. 1-4, 1995.

Imhof, W. L., D. L. Chenette, D. W. Datlowe, J. Mobilia, M. Walt, and R. R. Anderson, The correlation of AKR waves with precipitating electrons as determined by plasma wave and X-ray image data from the POLAR spacecraft, Geophys. Res. Lett., 289-292, 1998.

Imhof, W. L., R. R. Anderson, D. L. Chenette, J. Mobilia, S. M. Petrinec, and M. Walt, The correlation of rapid AKR variations with changes in the fluxes of precipitating electrons, Adv. in Sp. Res., 23, 1747-1752, 1999.

Imhof, W. L., M. Walt, R. R. Anderson, D. L. Chenette, J. D. Hawley, J. Mobilia, and S. M. Petrinec, Association of electron precipitation with auroral kilometric radiation, J. Geophys. Res., 105, 277-289, 2000.

Imhof, W. L., M. Walt, R. R. Anderson, J. D. Hawley, M. J. Brittnacher, S. M. Petrinec, and H. Matsumoto, Relationship between X-ray, ultraviolet, and kilometric radiation in the auroral region, J. Geophys. Res., 106, 10,479- 10,492, 2001.

Imhof, W. L., R. R. Anderson, M. Walt, J. D. Hawley, S. M. Petrinec, J. Mobilia, and H. Matsumoto, The dependence of AKR production on the intensity and energy spectra of auroral bremsstrahlung, J. Geophys. Res., accepted for publication, Manuscript Number: 2002JA009274, 2003.

Kaiser, M. L., and J. K. Alexander, Terrestrial kilometric radiation 3. Average spectral properties, J. Geophys. Res., 82, 3273, 1977a.

Kaiser, M. L., and J. K. Alexander, Relationship between auroral substorms and the occurrence of terrestrial kilometric radiation, J. Geophys. Res., 82, 5283, 1977b.

Kaiser, M. L., M. D. Desch, W. M. Farrell, J.-L. Steinberg, and M. J. Reiner, LF Band Terrestrial Radio Bursts Observed by Wind/WAVES", Geophys. Res. Lett., 23, 1283-1286, 1996.

Kasaba, Y., H. Matsumoto, K. Hashimoto, and R. R. Anderson, The angular distribution of auroral kilometric radiation observed by the Geotail spacecraft, Geophys. Res. Lett., 24, 2483-2486, 1997.

Kasaba, Y., H. Matsumoto, Y. Omura, R. R. Anderson, T. Mukai, Y. Saito, T. Yamamoto, and S. Kokubun, Statistical studies of plasma waves and backstreaming electrons in the terrestrial electron foreshock observed by Geotail, J. Geophys. Res., 105, 79-103, 2000.

Kokubun, S., T. Yamamoto, M. Acuna, K. Hayashi, K. Shiokawa, and H. Kawano, The GEOTAIL magnetic field experiment, J. Geomag. Geoelectr., 46,7,1994.

Liou, K., C.-I Meng, T. Y. Lui, P. T. Newell, M. Brittnacher, G. Parks, G. D. Reeves, R. R. Anderson, and K. Yumoto, On relative timing in substorm onset signatures, J. Geophys. Res., 104, 22807-22817, 1999.

Matsumoto, H., I. Nagano, R. R. Anderson, H. Kojima, K. Hashimoto, M. Tsutsui, T. Okada, I. Kimura, Y. Omura, and M. Okada, Plasma wave observations with GEOTAIL spacecraft, J. Geomag. Geoelectr., 46, 59-95, 1994.

Murata, T., H. Matsumoto, H. Kojima, A. Fujita, T. Nagai, T. Yamamoto, and R. R. Anderson, Estimation of tail reconnection lines by AKR onsets and plasmoid entries observed with GEOTAIL spacecraft, Geophys. Res. Lett., 22, 1849-1852, 1995.

Ogilvie, K. W., D. J. Chornay, R. J. Fitzenreiter, F. Hunsaker, J. Keller, J. Lobell, G. Miller, J. D. Scudder, E. C. Sittler, Jr., R. B. Torbert, D. Bodet, G. Needell, A. J. Lazarus, J. T. Steinberg, J. H. Tappan, A. Mavretic, and E. Gergin, SWE, A comprehensive plasma instrument for the WIND spacecraft, Space Sci. Rev., 71, 55-77, 1995.

Reiner, M. J., M. L. Kaiser, J. Fainberg, M. D. Desch, and R. G. Stone, 2Fp radio emissions from the vicinity of the Earth's foreshock: WIND observations, Geophys. Res. Lett., 23, 1247-1250, 1996.

Rostoker, G., J. C. Samson, F. Creutzberg, T. J. Hughes, D. R. McDiarmid, A. G. McNamara, A. Vallance Jones, D. D. Wallis, and L. L. Cogger, CANOPUS - A ground-based instrument array for remote sensing the high latitude ionosphere during the ISTP/GGS program, Space Sci. Rev., 71, 743-760, 1995.

Russell, C. T., R. C. Snare, J. D. Means, D. Pierce, D. Dearborn, M. Larson, G. Barr, G. Le, The GGS/Polar magnetic-fields investigation, Space Science Reviews, 71 (1-4), 563-582, 1995.

Steinberg, J.-L., C. Lacombe, and S. Hoang, A new component of terrestrial radio emission observed from ISEE-3 and ISEE-1 in the solar wind, Geophys. Res. Lett., 15, pp 176-179, 1988.

Steinberg, J.-L., S. Hoang, and J. M. Bosqued, Isotropic kilometric radiation: A new component of the Earth's radio emission, et al., Ann. Geophysicae, 8, pp 671-686, 1990.

Steinberg, J.-L., C. Lacombe, and S. Hoang, sounding the flanks of the Earth's bow shock to -230 Re: ISEE-3 observations of terrestrial radio sources down to 1.3 times the solar wind plasma frequency, *J. Geophys. Res.*, **103**, 23,565-23,579, 1998.

Steinberg, J.-L., C. Lacombe, P. Zarka, S. Hoang, and C. Perche, Terrestrial Low frequency bursts: escape paths of radio waves through the bow shock, Planetary and Space Science, submitted, 2003.

Voots, G. R., D. A. Gurnett, and S. -I. Akasofu, Auroral kilometric radiation as an indicator of auroral magnetic disturbances, J. Geophys. Res., 82, 2259, 1977.

Wu, C. S., and L. C. Lee, A theory of the terrestrial kilometric radiation, Astrophys. J., 230, 621, 1979.

e-mail:

roger-r-anderson@uiowa.edu and anderson@kurasc.kyoto-u.ac.jp,
matsumot@kurasc.kyoto-u.ac.jp, kozo@kurasc.kyoto-u.ac.jp, kojima@kurasc.kyoto-u.ac.jp,
kasaba@stp.isas.ac.jp, mkaiser@lepmlk.gsfc.nasa.gov,
bougeret@obspm.fr, steinberg@obspm.fr, and rostoker@space.ualberta.ca

Manuscript received February 20, 2003; revised June 16, 2003 ; accepted July 24, 2003 .